University of Massachusetts Medical School

eScholarship@UMMS

1998-09-10

Centrosome defects and genetic instability in malignant tumors

G A Pihan

Et al.

Let us know how access to this document benefits you.

Repository Citation

Centrosome Defects and Genetic Instability in Malignant Tumors[1]

German A. Pihan, Aruna Purohit, Janice Wallace, Hans Knecht, Bruce Woda, Peter Quesenberry, and Stephen J. Doxsey[2]

Department of Pathology [G. A. P., J. W., B. W.], Program in Molecular Medicine [A. P., S. J. D.], and Cancer Center [H. K., P. Q.], University of Massachusetts Medical School, Worcester, Massachusetts 06510

ABSTRACT

Genetic instability is a common feature of many human cancers. This condition is frequently characterized by an abnormal number of chromosomes, although little is known about the mechanism that generates this altered genetic state. One possibility is that chromosomes are missegregated during mitosis due to the assembly of dysfunctional mitotic spindles. Because centrosomes are involved in spindle assembly, they could contribute to chromosome missegregation through the organization of aberrant spindles. As an initial test of this idea, we examined malignant tumors for centrosome abnormalities using antibodies to the centrosome protein pericentrin. We found that centrosomes in nearly all tumors and tumor-derived cell lines were atypical in shape, size, and composition and were often present in multiple copies. In addition, virtually all pericentrin-staining structures in tumor cells nucleated microtubules, and they participated in formation of disorganized mitotic spindles, upon which chromosomes were missegregated. All tumor cell lines had both centrosome defects and abnormal chromosome numbers, whereas neither was observed in nontumor cells. These results indicate that centrosome defects are a common feature of malignant tumors and suggest that they may contribute to genetic instability in cancer.

INTRODUCTION

Faithful segregation of chromosomes into daughter cells is essential for maintaining the genetic stability of most organisms. Chromosome segregation is mediated by the mitotic spindle, which has a complex structural organization and precisely timed movements that ensure the accuracy of this process (reviewed in Refs. 1-5). In normal cells, the metaphase spindle is a bipolar structure comprised of microtubules that emanate from centrosomes at each pole with chromosomes aligned at the spindle center (6, 7). Although it is not completely understood how spindles are assembled, the centrosome appears to play an important role in the process (reviewed in Refs. 4 and 8). Spindle assembly and spindle-mediated movements during chromosome segregation are controlled, in part, by cell cycle regulators. These include a system of biochemical checkpoints, feedback controls, and degradation events that ensure the stepwise progression of mitotic events and, ultimately, the fidelity of chromosome segregation and the maintenance of genetic stability (1-3, 9-11). Genetic instability is a common feature of malignant tumors. It is frequently characterized by an abnormal number of chromosomes, a condition known as aneuploidy (12-14). Furthermore, recent results demonstrate that aneuploid cells exhibit continuous changes in chromosome number

throughout their lifetimes, suggesting that this CIN[3] may contribute to aneuploidy (15). These defects in chromosome number are thought to occur through missegregation of chromosomes (1, 15), but the mechanism by which this occurs has not been elucidated. It is easy to envision how defects in mitotic spindle organization and function could directly lead to chromosome missegregation (2, 3, 5, 16). Furthermore, because spindles are organized in part by centrosomes (4, 8, 17), it is possible that abnormal centrosome function could contribute to CIN. Support for this idea comes from a recent observation suggesting that centrosome number is amplified in genetically unstable cells mutant for the tumor suppressor p53 (18).

Centrosomes are comprised of a pair of centrioles, the duplication of which occurs once and only once during the normal cell cycle, and the surrounding pericentriolar material, the substance involved in microtubule nucleation (see Ref. 7). As an initial test of the idea that centrosome dysfunction may lead to chromosome missegregation through the organization of aberrant mitotic spindles, we examined centrosomes in malignant tumors and cell lines derived from tumors. We found that centrosomes immunolabeled with antibodies to pericentrin (19) were abnormal in structure, number, and function in a wide range of malignant tumors and tumor cell lines. Furthermore, tumor cell lines with abnormal centrosomes exhibited spindle abnormalities and high levels of CIN.

MATERIALS AND METHODS

Preparation of Archival Tissues. Archival tissue consisted of paraffin-embedded biopsy material fixed for 4-24 h in 10% formaldehyde in PBS. Samples used in this study were 2 weeks to 4 years old. Five-mm-thick tissue sections were cut on a conventional microtome used for paraffin-embedded tissue sectioning. Sections were floated on a water bath kept at 37°C, picked up on glass slides, allowed to air-dry, and baked at 60°C overnight. Sections were deparaffinized in xylenes (twice for 3 min each at room temperature) and placed in 100% ethanol. Sections were rehydrated in a descending gradient of ethanol-water to 70% ethanol, transferred to PBS, and kept at 4°C until immunostaining (see below).

Preparation of Cells from Fresh Tissues by Collagenase/DNase Digestion. Cell suspensions were prepared from surgical resection specimens of carcinomas and sarcomas by removing small samples (5 mm³) and mincing with a razor blade in PBS at room temperature. Minced tissue was washed in PBS and resuspended on an 1-ml aliquot of fresh PBS containing 1.0 unit/ml collagenase (Sigma Chemical Co.) and 0.1 unit/ml of DNase I (Sigma; Ref. 20). Tissue was rotated end-over-end for 2 h at room temperature. Samples were then strained in a 100-mm nylon filter (Nytex; Small Parts, Inc.). Cells were pelleted and washed in PBS by sequential centrifugation at 325 × g and then cytospun onto slides.

Cytospinning of Cells onto Slides. Suspension cells were collected by various methods (see below). Approximately 2 × 10⁵ cells were resuspended in 100 ml of PBS at room temperature and placed in a cytospin funnel (Shandon, Inc.). Cytofunnels were attached to slides and spun at room temperature for 5 min at 65 rpm in a clinical cytocentrifuge (Cytp 2; Shandon, Inc.). Cells on slides were fixed, processed, and mounted as described below.

[3] The abbreviations used are: CIN, chromosomal instability; DAPI, 4',6-diamidino-2-phenylindole; HD, Hodgkin's disease; pen/strep, 100 units/ml penicillin-0.1 mg/ml streptomycin; FISH, fluorescence *in situ* hybridization; MTOC, microtubule organizing center.

Antibodies. Antibodies to pericentrin (5 mg/ml, rabbit polyclonal) and α-tubulin (2 mg/ml, mouse monoclonal) were used as described (19, 21). To label spindles, we mixed antibodies to both proteins and incubated them with different secondary antibodies (Jackson ImmunoResearch Laboratories). DNA was visualized by staining with DAPI (Sigma).

Cell Lines. Tumor-derived cell lines were grown on coverslips (19) or fixed in formalin, embedded in paraffin, and sectioned. Most cell lines were obtained from American Type Culture Collection and grown as described. L428, KHM2, and JC are HD cell lines. They were obtained from the German Collection of Microorganisms and Cell Cultures (L428 and KHM2) and from an immunocompromised patient with a HD-like lymphoma (JC; grown in our laboratory). B115 and B218 are early-passage EBV-transformed lymphoblastoid B-cell lines from peripheral blood B lymphocytes (gift of J. Sullivan, University of Massachusetts Medical School, Worcester, MA). All lines listed above were grown in RPMI (Hyclone Laboratories), 20% FCS, and pen/strep. Breast carcinoma cell lines MDA-MB-436 and MDA-MB-157 were grown in Leibovitz L-15 medium with 20% FCS, insulin (0.25 units/ml), glucose (45 mg/ml), and pen/strep; BT-549 and HS578T were grown in RPMI 1640 with 10% FCS-pen/strep. The prostate cell line PC-13 was grown in RPMI with 10% FCS-pen/strep. Colon carcinoma cell lines HT-29 and Lovo were grown in McCoy's 5A medium with 10% FCS-pen/strep. All other cell lines above were grown in RPMI with 20% FCS-pen/strep (American Type Culture Collection).

Immunoperoxidase Labeling of Tissues and Cells for Centrosomes. Sections or cells on slides were pressure-heated in antigen retrieval solution (1 mM EDTA in water) in a microwaveable pressure cooker (Nordic Ware) for 20 min, allowed to cool to room temperature, and transferred to PBS (22). Slides were immersed in 3% H_2O_2 in PBS for 15 min to block endogenous peroxidase. Cells were then blocked in 2-nitro-5-thiobenzoate blocking buffer (TSA-Indirect kit; NEN Life Science Products) for 1 h, followed by standard indirect immunohistochemistry. Briefly, pericentrin antibody was diluted 1:1000 in TBB (See TSA-Indirect kit) and added to slides in 100-ml aliquots for 1 h at room temperature. Slides were washed in TNT (See NEN Life Science Products kit) 3 times for 5 min each. Biotinylated secondary antibody against rabbit immunoglobulins (Ventana Medical Systems) diluted 1:1000 was applied for 1 h and incubated as above. Slides were washed in TNT 3 times for 5 min each. Signals were amplified by catalyzed reporter deposition Tyramine signal amplification (Ref. 23; TSA-Indirect kit), following manufacturer's instructions. Slides were washed in TNT, counterstained in hematoxylin, and mounted in Permount (Sigma), as described by manufacturer.

Immunofluorescence Labeling of Tissues and Cells. Cells were grown on 12-mm glass coverslips or cytospun onto glass slides. Cells were washed in PBS by placing coverslips into 12-well plates (Costar) with 1–2 ml of PBS or by immersing slides in Coplin jars filled with PBS. Cells were permeabilized to release soluble proteins and better visualize centrosome staining (19). PBS was then aspirated, and permeabilization buffer [80 mM PIPES (pH 6.8), 5 mM EGTA, 1 mM $MgCl_2$, and 0.5% Triton X-100] was added to plates or Coplin jars and incubated for 60 s at room temperature. Coverslips or slides were transferred to new container/plate with −20°C methanol and incubated for 5 min. Samples were sometimes stored for days in methanol at −20°C. Cells were washed 5 times in PBS by replacing half of the volume and aspirating half of the volume. Blocking solution (1× PBS, 0.5% Triton X-100, and 2% BSA) was added, and cells were incubated for 10 min. Coverslips or slides were prepared for immunofluorescence microscopy as described (19). Immunofluorescence images were recorded on a Zeiss Axiophot using a ×100 objective on a Xillix charge-coupled device camera with a Kodak (KAF 1400) chip and then pseudocolored and merged using ITEX-IPL software. Immunoperoxidase images were recorded using ×60 and ×100 objectives in real color on an Olympus Vanox-S photomicroscope equipped with a Kodak CDS 460 digital camera.

Microtubule Nucleation and Centriole Labeling. To depolymerize and regrow microtubules, cells were treated with nocodazole and washed free of the drug as described (19, 21). To visualize centrioles, cells were treated with nocodazole, permeabilized with detergent (above) and processed for immunofluorescence using an α-tubulin antibody. Similar results were obtained with an antibody that selectively stains the polymerized form of tubulin (tyrosinated; gift of C. Bulinski, Columbia University).

FISH. Chromosome numbers were determined by FISH on interphase cells using centromeric probes specific for chromosomes 1 and 8, labeled directly with Spectrum Green (Vysis, Chicago, IL) or Spectrum Red as described (15, 24). Evaluation of chromosome numbers by FISH rather than conventional metaphase analysis was used so that cells could be examined at all cell cycle phases. Cells were grown on coverslips or cytospun onto glass slides, permeabilized in detergent, and fixed as for centrosome immunofluorescence. Probe hybridization and washes were as recommended by the manufacturer (Vysis). Nuclei were counterstained by DAPI (20 ng/ml, Sigma) in PBS, mounted (Vectashield, Vector Laboratories), and analyzed on a Zeiss epifluorescence microscope equipped with a triple-band pass filter cube, allowing the simultaneous visualization of Spectrum Green, Spectrum Red, and DAPI signals. Centromeric signals appeared as discrete dots in most cells or as elongated dots in cells presumed to be in the G_2 phase of the cell cycle. The numbers of red and green signals per cell were determined in 100–150 cells in each cell line in two separate experiments.

RESULTS

Defects in Pericentrin Organization in Tumors. We examined malignant tumors from a variety of tissues for the presence of centrosome defects. These included primary tumors of the breast, prostate, lung, colon, and brain, as well as metastatic tumors of the breast, lung, and colon. Tissue sections from archival formalin-fixed, paraffin-embedded material were reacted with antibodies to the centrosome protein pericentrin (19), and antibodies were detected by the amplified immunoperoxidase technique (23). The pericentrin antibody used in this analysis has been shown to specifically label centrosomes in a wide variety of cell types when used in combination with the immunofluorescence technique (19). We confirmed that the antibody produced a similar staining pattern by the immunoperoxidase technique in tissue sections and cells in culture. In normal interphase cells, a single brown dot was observed (the product of the immunoperoxidase reaction), and in mitotic cells, a pair of dots was detected, one at each pole of the spindle.

When tumors were analyzed at low magnification by immunoperoxidase staining, the tumor tissue could easily be delineated from adjacent nontumor tissue by the significantly higher level of pericentrin staining (Fig. 1). Higher magnification revealed that the pericentrin staining was organized into structures that were abnormal in size, shape, and number (Fig. 2, Tumor tissues). Most tumor cells had a single focus of pericentrin that was significantly greater in diameter than centrosomes in nontumor cells (3–10-fold greater). Tumor cells often had multiple pericentrin foci suggesting that supernumerary centrosomes were present in these cells (see below). Multiple foci were detected in both paraffin sections [Fig. 2, small arrowheads in A and D] and freshly prepared samples (Fig. 3H) and were sometimes interconnected by atypical filaments of pericentrin (Fig. 2O, arrowheads). These structural defects occurred together with variable levels of diffuse and patchy pericentrin material in the cytoplasm of tumor cells (Fig. 2, most panels).

The abnormal distribution of pericentrin staining seen in malignant tumors was not observed in nontumor tissues. We examined over 12 cell types in tissues adjacent to tumors including cells of tumor origin, resident cells in metastatic tumors, and cells in stroma, ducts, blood vessels, and smooth muscle [Fig. 2, Nontumor tissues (NT), arrowheads and large arrowheads in D, K, and N]. In all cases, a single discrete focus of pericentrin staining was detected, typical of the centrosome pattern in normal cells. A low level of diffuse staining was sometimes detected in nontumor tissues, which most likely represented the modest level of cytoplasmic pericentrin known to be present in normal cells. The absence of pericentrin anomalies in the many different types of nonneoplastic cells within tumor sections (for example, proliferating and nonproliferating cells, epithelial and endothelial cells, and so on) strongly suggests that this phenotype is tumor
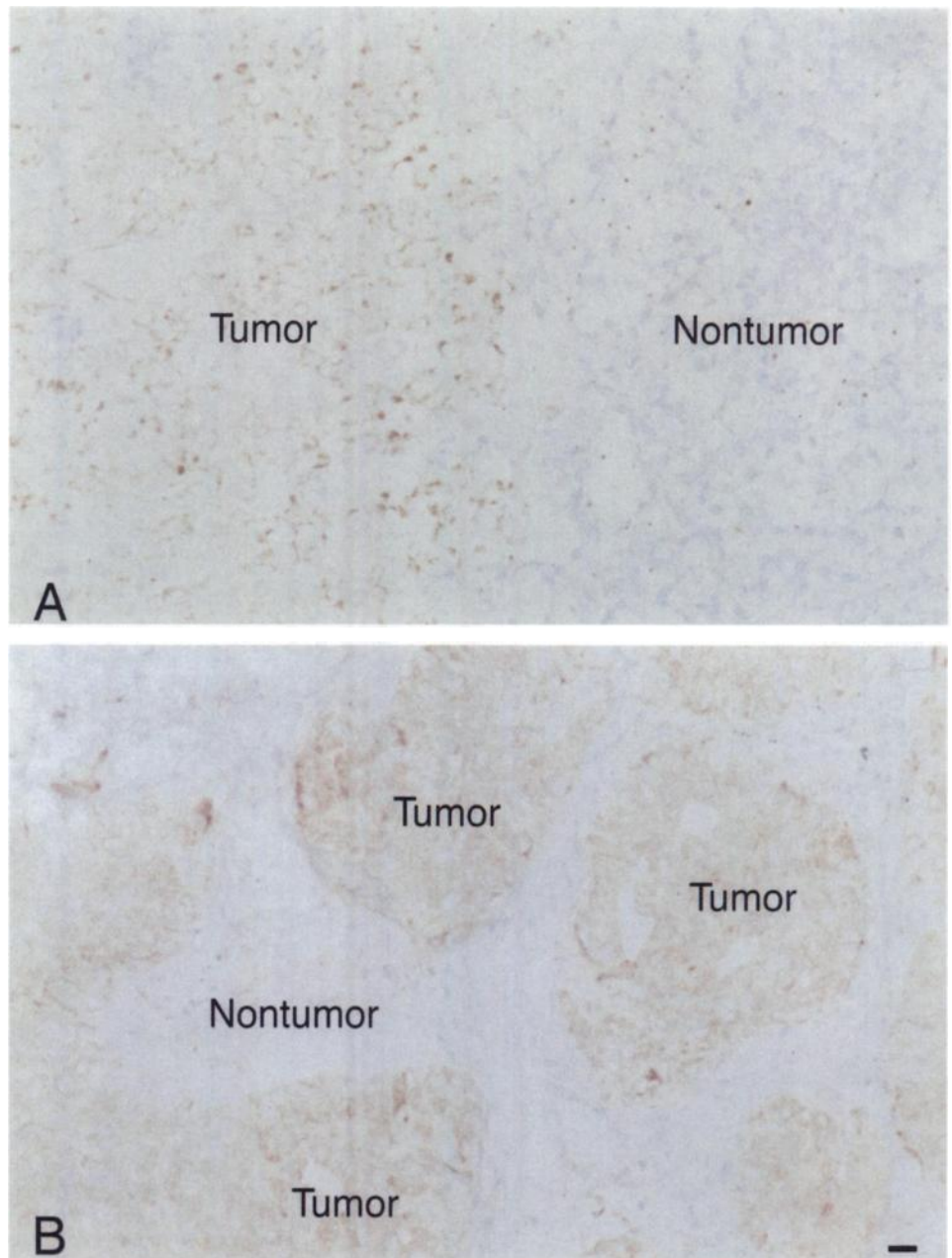
Fig. 1. Low-magnification images of malignant tumors showing amplified pericentrin staining. Paraffin-embedded tissue sections were stained for pericentrin by the immunoperoxidase method (*brown*) and counterstained with hematoxylin (*blue*) to reveal details of tissues and cells. Images show a high level of pericentrin staining in tumor tissue compared to nontumor tissue. *A*, breast adenocarcinoma metastasized to lymph node. *B*, lung tumor *in situ*. *Scale bar* (in *B*), 20 μm (for both *A* and *B*).

related and does not simply reflect the stage of differentiation, differences in cell type, or proliferation rate.

The presence of defective pericentrin structures in tumors was significantly higher than in nontumor tissues (Table 1, $P < 0.0001$, two-sided Fisher's exact test). Although nontumor tissues appeared normal in all cases, 93% of the tumors examined (81 of 87) showed one or more defects. Up to 95% of the cells in some tumors exhibited the abnormal phenotype. In some tumors, the abnormal phenotype was not observed. This could reflect a lower stage of tumor progression, the inability of our assay to detect subtle abnormalities in pericentrin organization, or the lack of centrosome abnormalities in these tumors. It appears that insensitivity of the archival tissue assay may be partially responsible for the apparent lack of defects in some tumors because pericentrin organization appeared to be more severely perturbed in freshly isolated cells from a limited number of tumors ($n = 5$; for example, see Fig. 3*H*). These data indicate that many malignant tumors have higher levels of pericentrin and that pericentrin

is organized into atypical and supernumerary structures in the cytoplasm of tumor cells.

Defects in Pericentrin Organization in Tumor-derived Cell Lines. The observed defects in pericentrin organization in malignant tumors were also found in permanent cell lines established from tumors. These included cell lines derived from colon, breast, and prostate and from patients with HD (Fig. 3). Using both immunoperoxidase and immunofluorescence methods, we detected pericentrin structures of abnormal size and shape (Fig. 3, *A*, *arrows*, *B*, and *D–G*) and supernumerary structures (Fig. 3, *A*, *arrowheads*, and *D–F*). Over 25 centrosomes were detected in some tumor-derived cells (Fig. 3*F*), and they varied in size from tiny flecks of material a fraction of the size of normal centrosomes to large aggregates (Fig. 3, *D* and *F*) or long linear arrays up to ten times larger than normal centrosomes (Fig. 3*G*). Diffuse cytoplasmic material was also observed in tumor cells and was usually found together with other centrosome defects (data not shown; see "Materials and Methods"). Up to 67% of the cells in
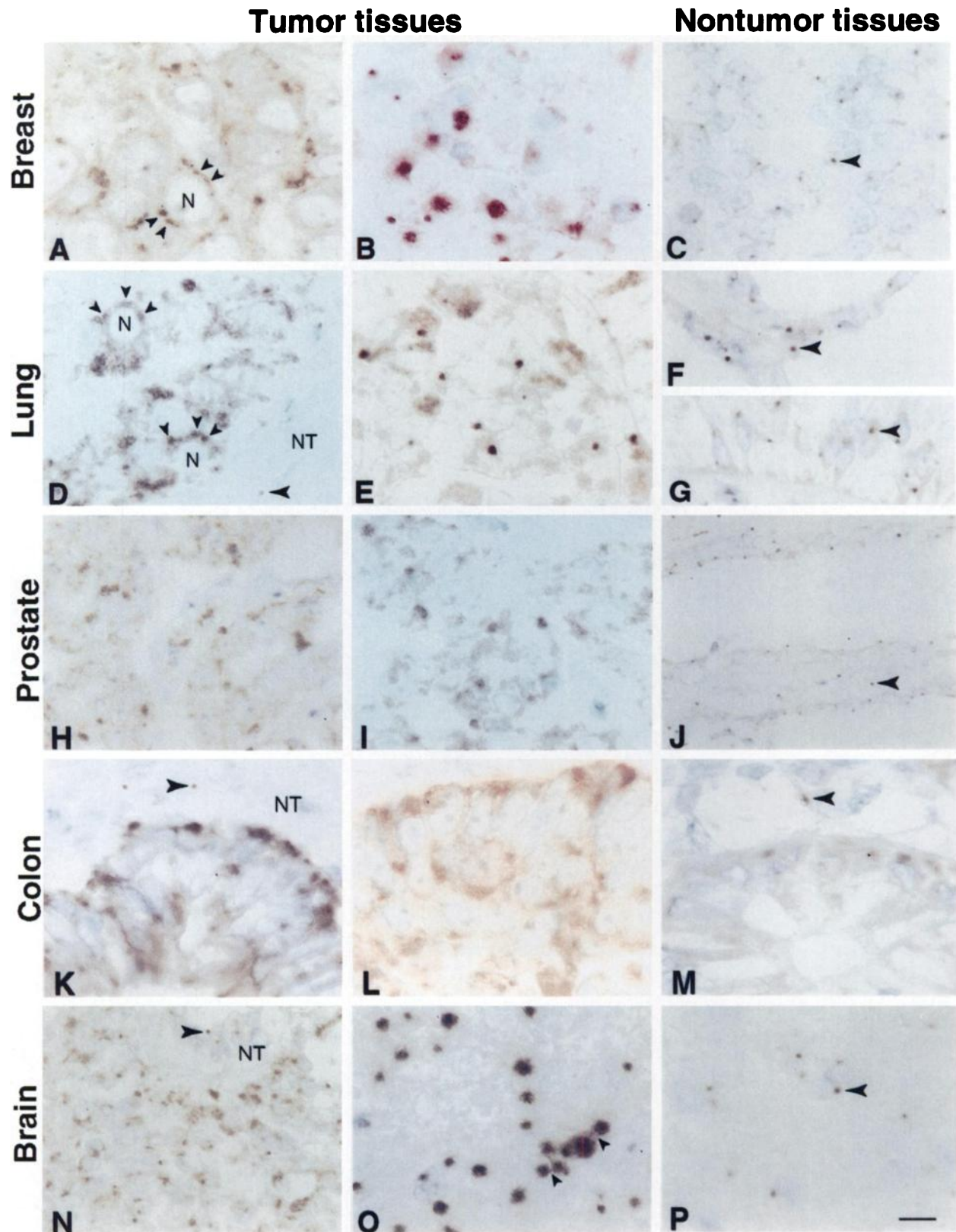
Tumor tissues   Nontumor tissues

Fig. 2. High-magnification images of malignant tumors showing abnormal pericentrin structures. Tissues were processed for pericentrin staining as in Fig. 1. Cells in nontumor tissues (*NT*), in the same tissue section as tumor cells (*T*), usually have a single small focus of staining, typical of normal centrosomes (*large arrowheads, Nontumor tissues*, and *NT* in *D, K*, and *N*). Pericentrin-staining structures in tumor cells are usually larger in diameter (most panels) and often abnormal in number (*A* and *D, small arrowheads*). In addition, most tumor cells contain increased levels of pericentrin within the cytoplasm (most panels). Occasionally, structures with abnormal morphology are observed (*O*, see linear elements at arrowheads). Tissues were from the following: *A–C*, lymph node with metastatic breast tumor; *D–G*, lung; *H–J*, prostate; *K–M*, colon; *N–P*, brain. Nontumor tissues were from the following: *C*, lymph node; *D (NT)*, stroma in lung; *F*, alveolar wall; *G*, bronchial epithelium; *J*, prostate gland; *K (NT)*, stroma in intestine; *M*, intestinal epithelium; *N (NT)*, blood vessel; *P*, brain white matter. *NT*, nontumor tissue; *N*, nucleus. All images are same magnification. *Scale bar* (in *P*), 10 µm (for *A–P*).
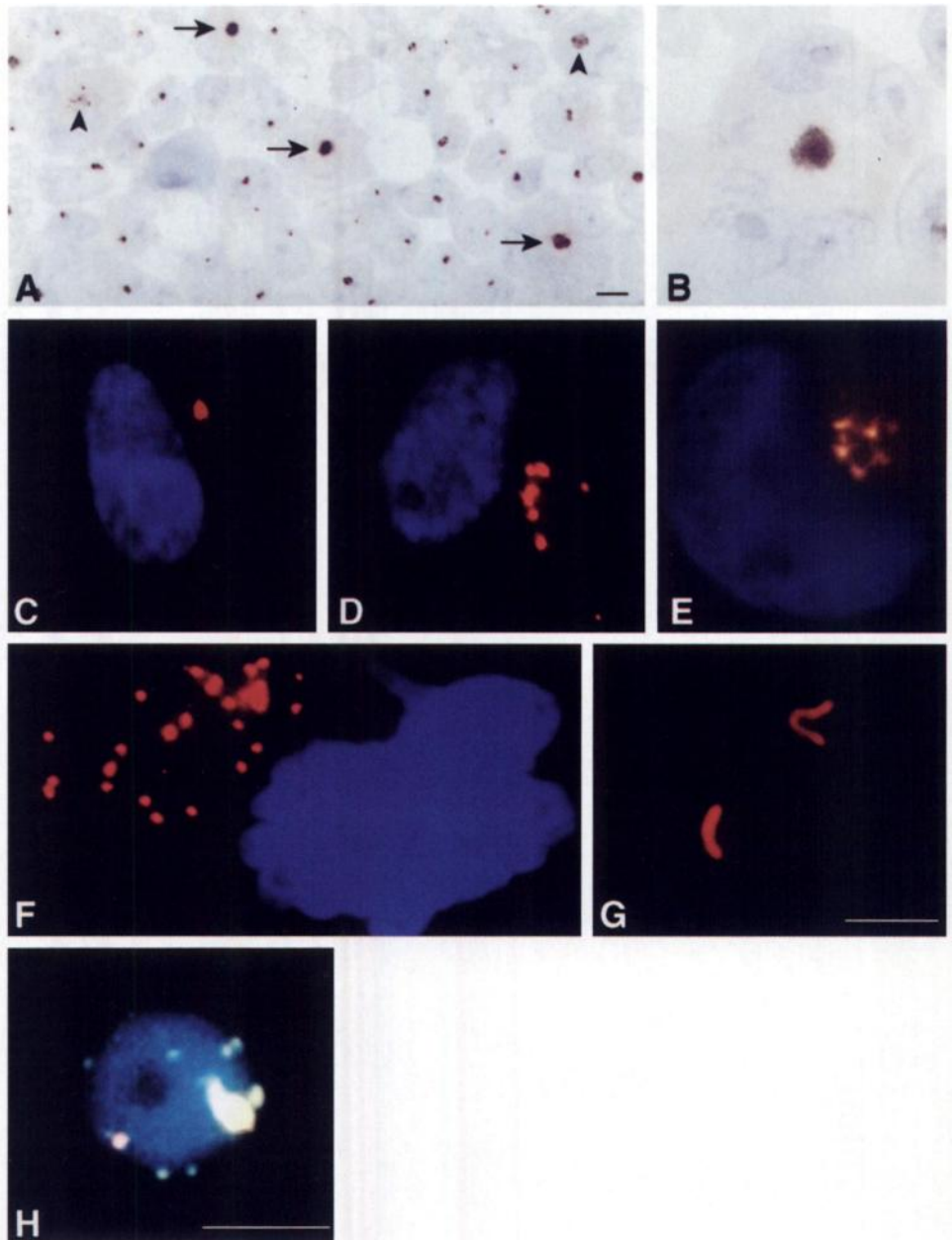
Fig. 3. Abnormal pericentrin structures in tumor-derived cell lines (A–G) and cells dissociated from tumors (H). A, HD cell line (L428) stained by immunoperoxidase (as in Fig. 1), showing several cells with enlarged pericentrin staining structures (arrows) and multiple pericentrin staining structures (arrowheads). B, enlargement of cell in A, showing large pericentrin structure at center of multiple nuclei. C, cell from a nontumor cell line (B218) processed for immunofluorescence with antipericentrin antibodies and showing a single dot (red) next to the nucleus (blue), typical of centrosome staining in normal cells. Cells from breast tumor cell lines (D, MDA-MB-157; F, BT-549) and a prostate tumor cell line (E and G, PC-13) showing multiple pericentrin staining structures (5 to >25). In addition, the structures are variable in size (D and F), linked together by strands of pericentrin-staining material (E) and organized into string-like arrays (G, nucleus out of view). H, cell dissociated from a human breast tumor showing multiple fluorescent foci of pericentrin staining (white/yellow). Scale bars, 10 μm (scale bar in G for B–G. A and B, immunoperoxidase labeling; C–H, immunofluorescence labeling. A–G, cell lines; H, cell dissociated from tumor.

some tumor-derived lines had defective pericentrin structures, whereas most cells from nontumor lines had single fluorescent dots of uniform size, typical of pericentrin staining in normal cells (Fig. 3C). Statistical analysis demonstrated that the defects observed in all eight tumor lines examined were significantly greater than those in nontumor cell lines (Table 2, all Ps <0.001, Pearson's χ2 test). Nontumor cells rarely exhibited multiple pericentrin foci. It is possible that nontumor cells in both established lines and primary tumors exhibit a

Table 1 Centrosome abnormalities in malignant tumors[a]

Abnormal centrosomes[b]	Tumor type[c]				
	Breast	Prostate	Brain	Lung	Colon
In tumor cells	18/19	16/18	19/20	15/15	13/15
In nontumor cells[d]	0/21	0/25	0/18	0/23	0/20

[a] For all samples in this analysis, paraffin-embedded tissues were sectioned, reacted with pericentrin antibodies and immunoperoxidase methods, and examined by light microscopy. Defects in centrosomes were statistically higher in tumors as compared to nontumor cells. Statistical analyses were described in "Results" and "Discussion."

[b] Centrosomes were considered abnormal if they had diameters >2 times the diameter of centrosomes in nontumor control cells in the same section; if they lacked centrioles; if they were present in more than two copies per cell; or if they were organized into elongated structures >3 μm long, string-like elements, or large patchy aggregates. Most tumor cells had more than one defect. Similar results were obtained by immunofluorescence analysis (data not shown).

[c] Tumors were identified by architectural and nuclear cytological features on hematoxylin-counterstained immunoperoxidase preparations.

[d] Nontumor cells had none of the centrosome abnormalities described above. They were used as internal controls for each tumor and included stromal cells, lymphocytes, astroglia, endothelial cells, and mature nonneoplastic epithelial cells present within the same tumor tissue sections. Centrosomes in nontumor cells were indistinguishable from those of normal cells.

Table 2 *Aberrant centrosomes, nuclei, and chromosome numbers in tumor- and non-tumor-derived cell lines*[a]

Cells and cell lines[b]	Tissue of origin	Abnormal centrosomes[c]	Abnormal Nuclei[d]	Chromosomal instability (Chr1/Chr8)[e]
Tumor-derived cell lines				
HT-29	Colorectal	24%	12%	57%/43%[f]
Lovo	Colorectal	9%	11%	ND[g]/27%[f]
HS578T	Breast	22%	15%	66%/70%
BT-549	Breast	67%	50%	73%/72%
MDA-MB-436	Breast	14%	17%	36%/40%
L428	HD	16%	26%	33%/29%
KHM2	HD	45%	29%	37%/28%
JC	HD	13%	11%	29%/29%
Non-tumor-derived cell lines				
B115	Lymphoblastoid	3%	2%	6%/5%
B218	Lymphoblastoid	2%	3%	7%/4%
COS 7	Monkey kidney	0.3%	0.5%	ND

[a] Defects in centrosomes, nuclei, and chromosome number were all statistically higher in tumor cells as compared to nontumor cells. Statistical analyses were performed as described in "Results" and "Discussion."

[b] Cell lines were described in "Materials and Methods."

[c] The percentage of cells with three or more discrete pericentrin-staining foci, pericentrin structures without centrioles, long linear structures (>3 μm long), and structures much smaller (<50%) or larger (>300%) in diameter than in control cells. All cells were examined by immunofluorescence methods. At least 500 cells were counted for each cell line. Values represent the average of three independent experiments. Similar results were obtained by immunoperoxidase labeling (data not shown).

[d] The percentage of cells with nuclei exhibiting defects in morphology and/or size (multilobed or multinucleate), as observed by DAPI staining. At least 300 cells were counted for each cell line and values represent the average of two experiments.

[e] Percentages represent the fraction of cells with chromosome numbers that were different from the mode (a gain or loss), as described (15). We used directly labeled chromosome-specific centromeric probes to chromosome 1 (Chr1) and chromosome 8 (Chr8). Between 100 and 150 cells were counted for each value, which is the average of two staining reactions.

[f] Previously determined values for chromosomal instability (15).

[g] ND, not determined.

basal level of pericentrin abnormalities that is corrected through appropriate cell cycle checkpoints or eliminated by activation of appropriate apoptotic pathways (see Refs. 1 and 11).

Supernumerary Centrioles and Acentriolar Structures in Tumor-derived Cell Lines. If the atypical pericentrin structures described above were centrosomes with normal architecture, they should possess centrioles (see Ref. 7). To detect centrioles, cells were stained with antibodies to α-tubulin following the selective depolymerization of cytoplasmic microtubules with nocodazole (7, 19). To our surprise, centrioles in tumor cells were sometimes absent from pericentrin structures, especially those of variable size and irregular shape (Fig. 4, *C* and *D*, *large arrowhead*). However, pericentrin structures of normal size and morphology usually had centrioles, even when they were present in multiple copies in the cytoplasm of tumor cells (Fig. 4, *E* and *F*) and cells dissociated from fresh tumors (data not shown). Control cells typically had a pair of centrioles at the focus of pericentrin staining, as expected for normal cells (Fig. 4, *A* and *B*).

Quantitative analysis showed a good correlation between centrioles and pericentrin foci in control cells (100%, *n* = 214), whereas centrioles were absent from pericentrin structures in a significant percentage of cells in a breast line (11.2%, *n* = 223, BT-549), a HD line (14.1%, *n* = 227, L428), and others (data not shown). This demonstrates that, although many pericentrin-staining structures observed in tumors and tumor-derived cell lines are canonical centrosomes, a proportion of them lack centrioles. Because pericentrin is found in centrosomes and other MTOCs that lack centrioles (19), we examined all pericentrin structures in tumor cells for the ability to nucleate microtubules.

All Pericentrin Structures in Tumor Cell Lines Nucleate Microtubules. To test for microtubule nucleation, cells were treated with nocodazole to depolymerize microtubules and were washed free

of the drug to allow microtubule regrowth from centrosomes. Under these conditions, essentially all pericentrin foci nucleated the growth of new microtubules regardless of their number, size, morphology, and the presence of centrioles (Fig. 5). Even the smallest detectable specks of material (Fig. 5, *C* and *E*) and the long linear arrays (Fig. 5*G*) nucleated microtubules (Fig. 5, *D*, *F*, and *H*). These additional MTOCs significantly increased the nucleating capacity of tumor cells compared to control cells, in which a single centrosome (one or two dots) nucleated a single microtubule aster (Fig. 5, *A* and *B*). The presence of multiple MTOCs suggested that tumor cells might form abnormal spindles during cell division.

Defects in Mitotic Spindle Organization and Chromosome Segregation in Tumor Cell Lines. Spindle defects were observed in cells of all tumor-derived lines (Fig. 6) and cells freshly dissociated from tumors (data not shown). Although control cells had a typical bipolar spindle with a single pericentrin focus at each pole (Fig. 6, *A-C*), tumor cells often had misshapen spindles and spindles with poorly focused poles or multiple poles (Fig. 6, *E*, *H*, *K*, and *N*). Most abnormal spindles were associated with pericentrin structures that were aberrant in number (Fig. 6, *D-F*, *G-I*, and *M-O*), shape (Fig. 6, *M-O*), and orientation (Fig. 6, *D-F*, *G-I*, and *J-L*).

In many tumor cells, unequal numbers of chromosomes were aligned between multiple poles of abnormal spindles (Fig. 6, *I* and *O*), and they appeared to be missegregated as cells divided (Fig. 7). We often observed telophase cells undergoing multipolar divisions and segregating their genomes unequally into more than two progeny (Fig. 7, *A* and *B*). In other telophase cells, chromosomes appeared to remain at the metaphase plate after others had been segregated to the poles (Fig. 7*E*, *arrow*) or they segregated part way but did not appear to be included in reforming nuclei (data not shown). Abnormalities in spindle organization and function were detected in up to 36% of mitotic cells in some tumor cell lines (for example, BT-549, *n* = 143). These observations demonstrate that defects in pericentrin organization, spindle structure, and chromosome segregation often occur together in the same tumor cell, and they suggest that centrosome and spindle defects contribute to abnormal partitioning of chromosomes. To obtain a more accurate measure of chromosome missegregation, we examined the copy number of individual chromosomes in tumor cells.

CIN and Nuclear Abnormalities in Tumor Cell Lines. To assay for CIN in tumor cells, we examined chromosomes in individual cells by FISH (24) using probes for chromosomes 1 and 8. In all malignant tumor cell lines examined, we found a dramatic variability in chromosome copy number among individual cells in the population. One such example is shown in Fig. 8, where the frequency distribution of chromosomes 1 and 8 in a malignant breast carcinoma cell line (Fig. 8, *C* and *D*, BT-549) clearly demonstrates a highly variable number of chromosomes per cell. In contrast, a nontumorigenic cell line (Fig. 8, *A* and *B*, B115) has only two copies of each chromosome in most cells. The variability in chromosome number observed in tumor cells has recently been termed CIN (15) and is thought to result from chromosome missegregation during mitosis. Over 70% of the cells in some lines exhibited CIN of chromosomes 1 and 8, with copy numbers ranging from 1 to 22 per cell (Fig. 8 and Table 2). The level of CIN in all tumor cell lines examined (27–73%) was statistically higher than that in control cells (Table 2; 4–7%, $P < 0.001$, Pearson's χ^2 test). Control cells used in this study had CIN levels similar to those of uncultured lymphocytes and to those used in other studies (15) and, thus, appeared to represent the intrinsic error rate of the FISH methodology. Despite the fact that the number of tumor cell lines used in this analysis was low (*n* = 8), we found a positive correlation between abnormal pericentrin organization and insta-
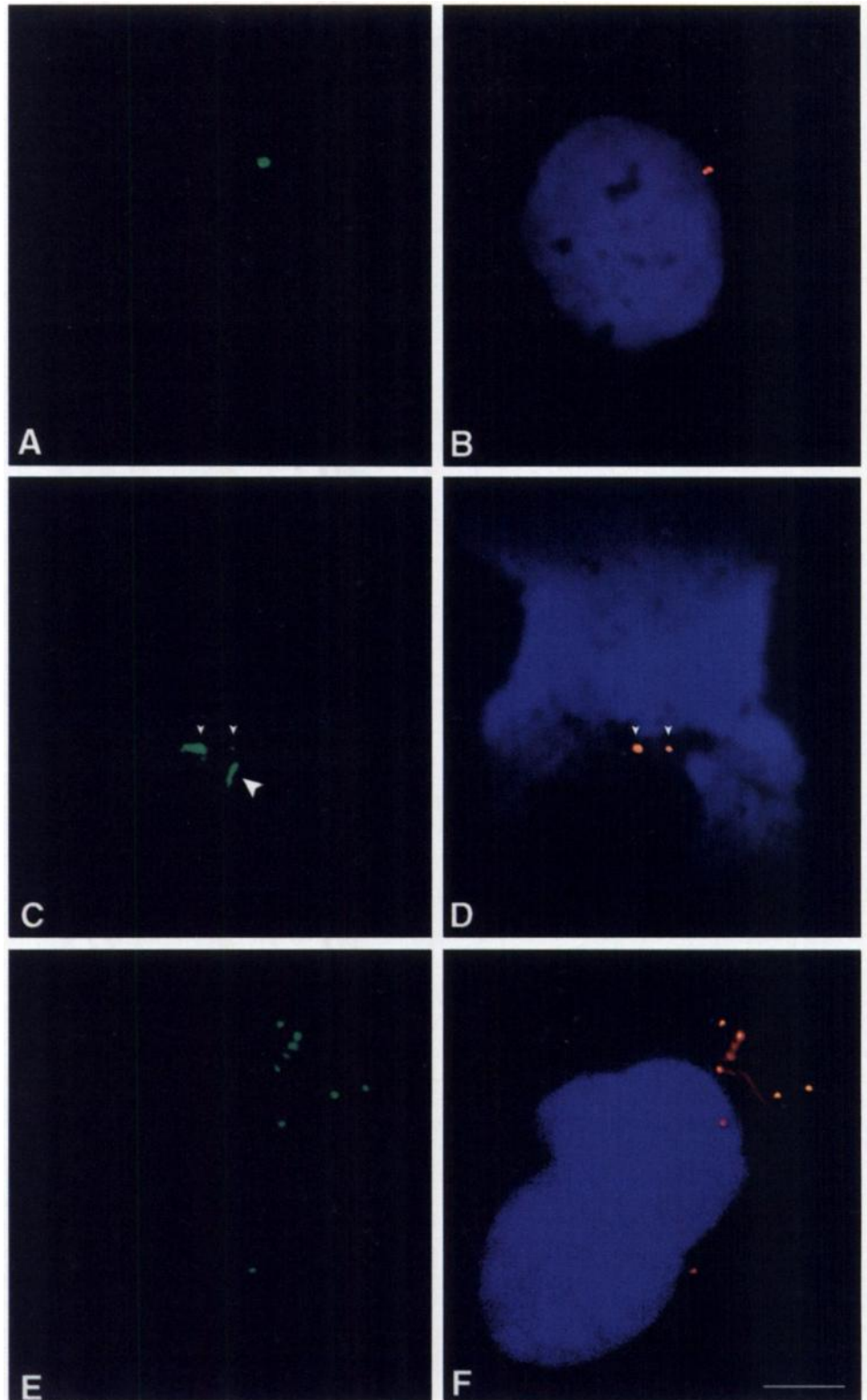
Fig. 4. Supernumerary centrioles and acentriolar structures in tumor-derived cell lines. Centrioles were labeled with an α-tubulin antibody following depolymerization of cytoplasmic microtubules by nocodazole (see "Materials and Methods"). Horizontal series are of the same cell in all cases. In control cells (B115), a pair of centrioles (B) is found at the focus of pericentrin staining (A). In the HD cell line (L428) the two separated centrioles (D, arrowheads) are coincident with some pericentrin staining foci (C, small arrowheads) but not with others (C, large arrowhead). A cell from a breast tumor cell line (BT-549) with multiple foci of pericentrin staining is shown in E, each coincident with centriole staining (F). A few microtubules that were incompletely depolymerized are present in F. Scale bar (in F), 10 μm (for A–F).

bility of chromosome 1 ($P < 0.05$, Spearman's rank correlation) but not chromosome 8 ($P = 0.204$, see "Discussion"). In addition, aberrant nuclei (multilobed or multinucleate) were observed in all tumor cell lines (Fig. 3, E and F, and Table 2), and their presence correlated with abnormal pericentrin organization ($P < 0.001$, Pearson's $\chi 2$ test). Taken together, these results indicate that centrosome defects and CIN occur together in most malignant tumor cell lines.

DISCUSSION

Using immunoperoxidase and immunofluorescence labeling techniques and antibodies to pericentrin, we have identified widespread defects in centrosomes in the most common human malignant tumors and tumor-derived cell lines. These tumor cells missegregate chromosomes on aberrant mitotic spindles and exhibit variability in chromosome number. Given the important role of
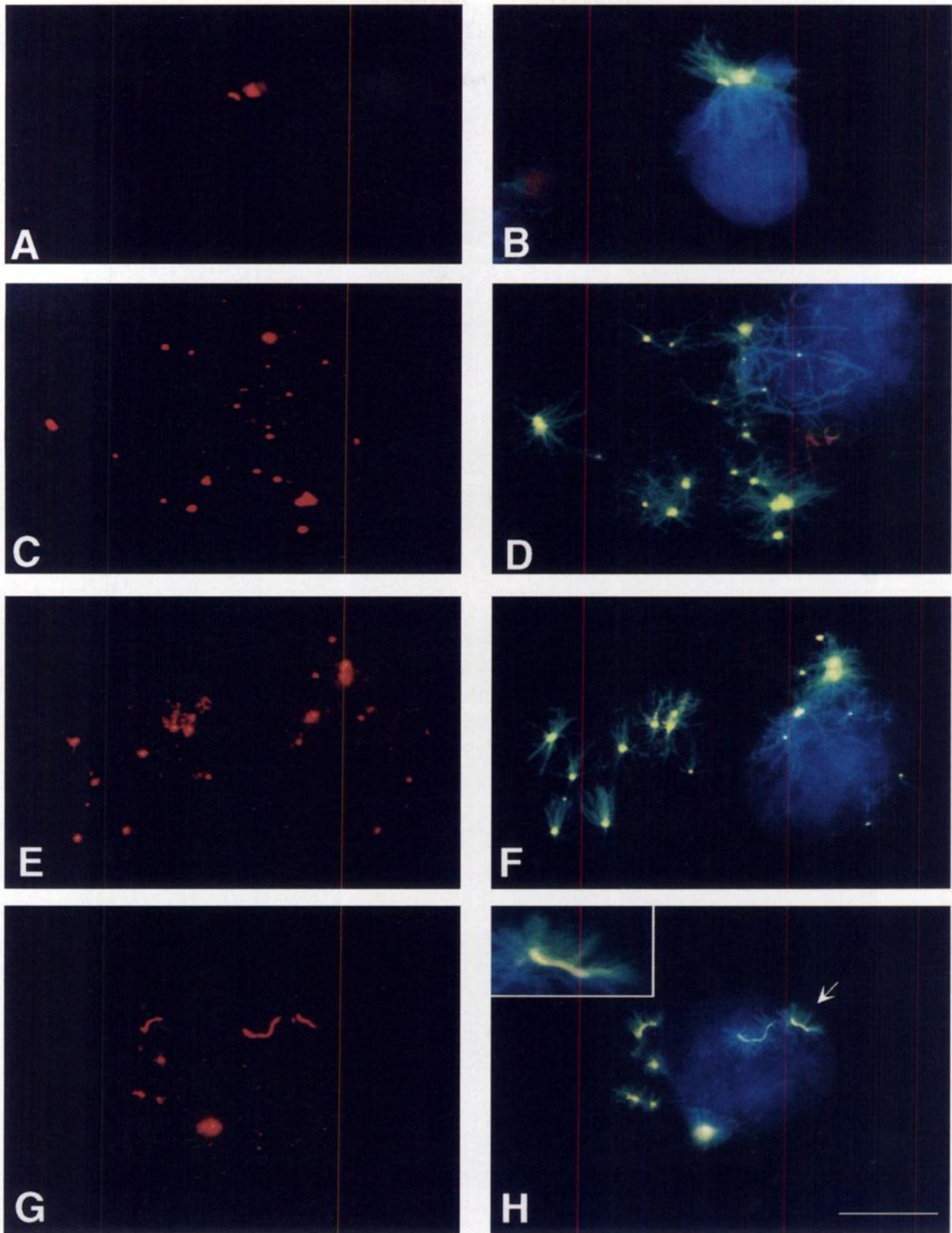
Fig. 5. All pericentrin-staining material nucleates microtubules. Cells from the control cell line B115 (*A* and *B*) and breast cancer-derived cell lines, BT-549 (*C*, *D*, *G*, and *H*) and MDA-MB-436 (*E* and *F*) were treated with nocodazole to depolymerize microtubules, washed, and allowed to regrow microtubules. Cells were triple-labeled for pericentrin (*red* or *yellow*), microtubules (*green*), and DNA (*blue*). All foci of pericentrin staining (*A*, *C*, *E*, and *G*) nucleated the growth of microtubules (*B*, *D*, *F*, and *H*). Even the very small foci seen in *C*, *E*, and *G* and the atypical elongated elements in *G* nucleated microtubules (*D*, *F*, and *H*). *Inset* (in *H*), higher magnification of region at *arrow*. All ectopic nucleating centers are in a single cell as determined by phase contrast microscopy (data not shown). *A*, *C*, *E*, and *G*, pericentrin staining; *B*, *D*, *F*, and *H*, triple-channel overlay showing pericentrin (*yellow*), microtubules (*green*), and DAPI (*blue*). *Scale bar* (in *H*), 10 μm (for *A–H*). Horizontal series (*A* and *B*; *C* and *D*; *E* and *F*; *G* and *H*) are of the same cell.
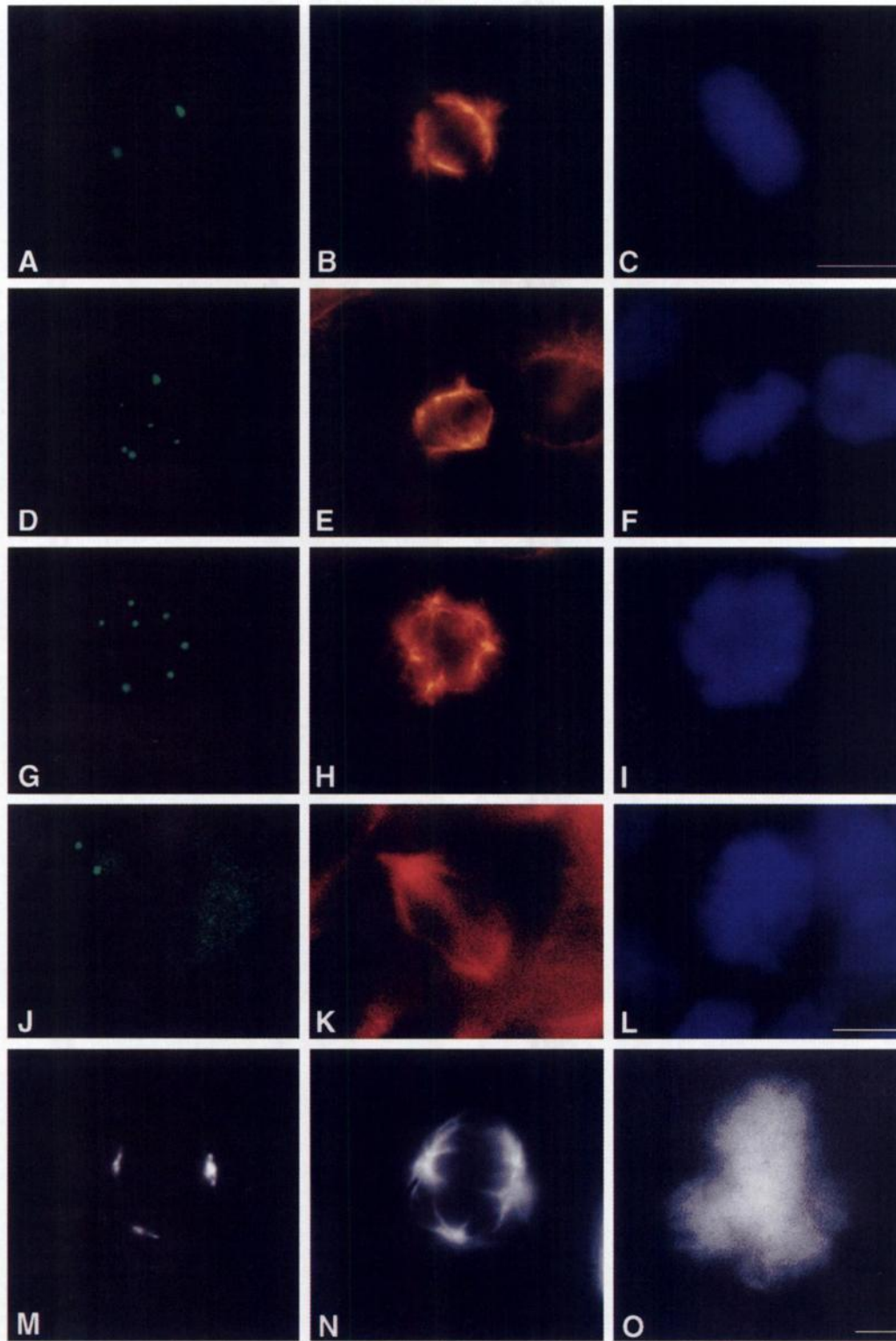
Fig. 6. Abnormal pericentrin structures are associated with aberrant spindles. Control cell (B115) with two centrosomes (A) at the poles of a normal bipolar spindle (B) and DNA aligned on the metaphase plate (C). Abnormal pericentrin structures and spindle defects in cell lines derived from a breast tumor (BT-549, D–I), a prostate tumor (PC-13, J–L), and an individual with HD (M–O). Cells with pericentrin structures of variable sizes, shapes, and numbers participate in the formation of multipolar spindles (G, H, M, and N) and spindles with unfocused or misshapen poles (D, E, J, and K). Some pericentrin structures do not localize to the poles of aberrant spindles (D, E, G, and H). A, D, G, and J, pericentrin structures; B, E, H, and K, microtubules; and C, F, I, and L, DNA. Horizontal series (A–C; D–F; G–I; J–L) are of the same cell. Scale bars, 10 μm (scale bar in C for A–C, in L for D–L; in O, for M–O).

centrosomes in mitotic spindle organization, it is possible that centrosome defects contribute to this CIN and, ultimately, to the neoplastic phenotype.

Although tumor cells derived from different tissue sources have

defects in different biochemical pathways (25), it is remarkable that nearly all malignant tumors examined in this study exhibited abnormal centrosomes. Abnormal centrosome features included structural defects, the absence of centrioles, elevated levels of pericentrin staining, super-
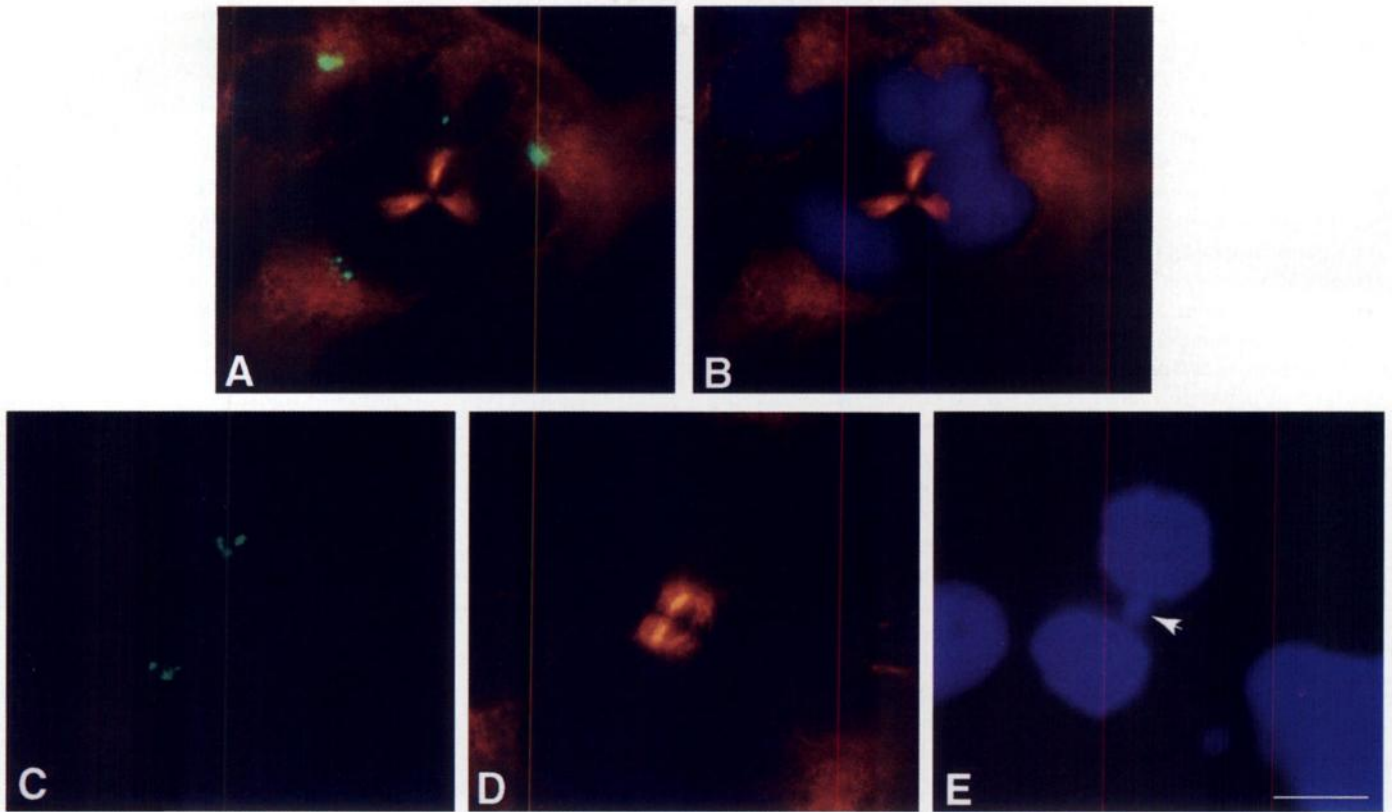
Fig. 7. Aberrant spindles missegregate chromosomes. A telophase cell from the prostate cancer cell line (PC-13) showing a tripolar spindle (*B*) with three spindle poles (*A*), some with multiple pericentrin structures (*A, bottom left* and *top right*). Chromosomes are segregated into three nascent daughter cells (*B*; note midbodies, the remnants of the spindle). Another telophase cell from a breast cancer cell line (BT-549, *C–E*) with multiple centrosomes at both poles (*C*) and typical midbody staining of microtubules (*D*) is shown. Missegregated chromosome(s) remain between reforming nuclei of daughter cells (*E, arrow*). *Green/yellow,* centrosomes; *red,* microtubules; *blue,* DNA. *A,* superposition of centrosomes and microtubules; *B,* superposition of microtubules and DNA. *Bar* (in *E*), 10 μm (for *A–E*). Horizontal series (*A* and *B*; *C–E*) are of the same cell.

numerary structures, and increased microtubule nucleation. In contrast, centrosomes in nontumor cells were consistent in size, shape, and number and indistinguishable from those of other normal cells (19). These observations clearly demonstrate that the centrosome-defective phenotype is tumor related.

The presence of centrosome defects correlated remarkably well with chromosome instability because both were significantly higher in tumor *versus* nontumor cells ($P < 0.001$, Pearson's $\chi2$ test). Furthermore, we often observed missegregated chromosomes and defective centrosomes in the same mitotic cells, suggesting a direct relationship

Fig. 8. CIN in tumor and nontumor cell lines. Frequency distribution of chromosomes 1 (*A* and *C*) and 8 (*B* and *D*) in a control cell line (B115, *A* and *B*) and in the breast cancer cell line (BT-549, *C* and *D*), as determined by quantitative analysis of cells stained by FISH. The copy number of chromosomes 1 and 8 are different from the mode in ~70% of the cells in BT-549 and <5% in B115. B115, mode = 2 for both chromosomes; BT-549, mode = 4 for chromosome 1 and mode = 5 for chromosome 8.
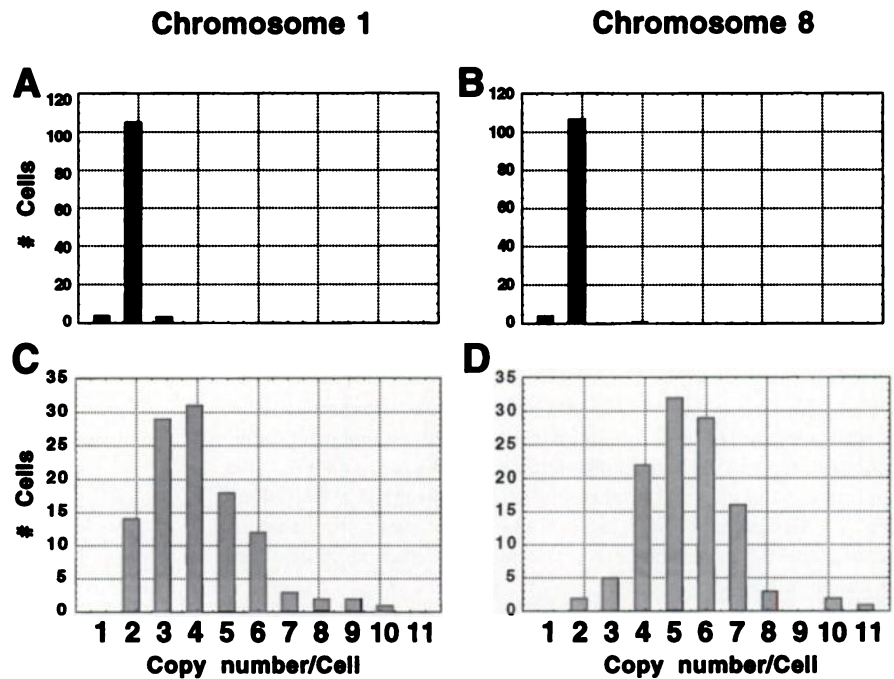
between these two cellular anomalies. In addition, we observed a statistically significant correlation between the level of centrosome defects and the level of chromosome 1 instability in tumor cells ($P < 0.05$, Spearman's rank correlation).

Although these data show a correlation between centrosome defects and CIN in tumor cell lines, they do not demonstrate that centrosomes play a direct role in the generation of CIN. Perhaps the most compelling data supporting a role for centrosomes in this process comes from transient transfection experiments showing that overexpression of a single centrosome protein (pericentrin) induces the formation of abnormal centrosomes, assembly of disorganized spindles and variability in chromosome numbers (CIN; Ref. 26). These aberrant features of pericentrin overexpressing cells are strikingly similar to those observed in malignant tumor cells. We are currently analyzing the pericentrin overexpressing cells for tumorigenic properties *in vitro* and *in vivo* (27–29).

It is easy to envision how a primary centrosome defect could contribute to CIN and, perhaps, to the development of the neoplastic phenotype. We propose a model in which centrosome defects alter the normal assembly, organization, and function of mitotic spindles, leading to the missegregation of chromosomes. These events could result in gains and losses of chromosomes that, together with the growth-selection pressure that tumors experience, provide a mechanism by which cells could accumulate tumor-promoting genes (activated oncogenes) and lose normal copies of tumor suppressor genes. Cells with these genetic defects would be predisposed to the acquisition of additional genetic lesions that could lead to the malignant neoplastic phenotype (1, 15). If centrosome defects are involved in tumorigenesis, they should appear early in tumorigenesis. We are currently examining early-stage cancers for centrosome anomalies.

The ability to induce chromosome instability through the artificial elevation of pericentrin (and perhaps other centrosome proteins) raises the possibility that a similar mechanism may be operating in tumor cells. Consistent with this idea is the universally higher levels of pericentrin staining observed in malignant tumors. Assembly of this excess protein could induce the formation of the ectopic microtubule nucleating centers and aberrant mitotic spindles that are commonly observed in tumor cells. Assembly of these multiple atypical MTOCs could occur without invoking multiple rounds of centriole duplication (18) because structures that lack centrioles and retain the capacity to nucleate and organize microtubules are found in cells of many organisms (30–33).

The centrosome defects observed in tumor cells could also arise indirectly through disruption of other cellular processes such as cytokinesis or through abrogation of cell cycle regulatory pathways such as cell cycle checkpoints that allow mitosis to proceed even when DNA is damaged or when chromosomes are improperly aligned on the spindle (see below; Refs. 1, 2, 9–11, and 34). Although cytokinesis failure may occur in some tumor cells, we believe that it cannot account for the centrosome defects observed in this study. Multiple rounds of failed cytokinesis should produce cells with structurally normal centrosomes, the numbers of which reflect multiple doublings (2 to 4 to 8, and so on; Ref. 35). However, centrosomes in tumor cells were highly variable in number and had numerous structural defects. Furthermore, cells that fail in cytokinesis should exhibit strict duplications of the genome (tetraploid, octaploid, and so on) rather than the enormous variability in chromosome number observed in this study (Fig. 8). These observations indicate that cytokinesis failure alone is insufficient to explain the defective centrosome phenotype observed in tumor cells.

Little is known about how the mammalian centrosome duplicates and assembles to form a functionally mature organelle. Results from embryonic systems have shown that centrosome duplication

and assembly continues when the cell cycle is blocked (36, 37) and when DNA replication is arrested (7, 35). However, recent work suggests that the centrosome duplication cycle may be controlled by the tumor suppressor gene *p53*, which is involved in regulating cell cycle checkpoints at both G_1-S and G_2-M (18, 38, 39). In addition, other genes are likely to control this process (see Refs. 7 and 30). It does not appear that the centrosome abnormalities observed in this study result from abrogation of p53 function because some cancer cell lines used in our analysis (Lovo) exhibit centrosome defects and CIN but have normal levels of functional p53 (15). Duplication of centrioles in mammalian cells and the spindle pole body in yeast begins around the time of the G_1-S transition (start, restriction point; see Refs. 7 and 30). Although the regulatory pathways that control this transition are likely to play a role in centriole duplication in mammalian cells, it is not until late in G_2 that two functionally active centrosomes appear. This suggests that additional regulatory controls are involved in the assembly and functional maturation of centrosomes. A more detailed analysis of the centrosome-defective phenotype in malignant tumors using high-resolution microscopy (40) and other methods may provide insights into the mechanisms of centrosome assembly and maturation and may also provide a better understanding of the relationship between centrosome defects and chromosome missegregation in cancer.

ACKNOWLEDGMENTS

Note Added in Proof

Similar centrosome defects were recently described in breast carcinoma (W. Lingle, W. H. Lutz, J. Ingle, N. J. Maihle, and J. L. Salisbury, Proc. Natl. Acad. Sci. USA, *95:* 2950–2955, 1998.)

REFERENCES

1. Hartwell, L. H., and Kastan, M. B. Cell cycle control and cancer. Science (Washington DC), *266:* 1821–1828, 1994.
2. Rudner, A. D., and Murray, A. W. The spindle assembly checkpoint. Curr. Opin. Cell Biol., *8:* 773–780, 1996.
3. Wells, W. A. The spindle assembly checkpoint: aiming for a perfect mitosis, every time. Trends Cell Biol., *6:* 228–234, 1996.
4. Waters, J. C., and Salmon, E. Pathways of spindle assembly. Curr. Opin. Cell Biol., *9:* 37–43, 1997.
5. Nicklas, R. B. How cells get the right chromosomes. Science (Washington DC), *275:* 632–637, 1997.
6. McIntosh, J. R., and Koonce, M. P. Mitosis. Science (Washington DC), *246:* 622–628, 1989.
7. Kellogg, D. R., Moritz, M., and Alberts, B. M. The centrosome and cellular organization. Annu. Rev. Biochem., *63:* 639–674, 1994.
8. Merdes, A., and Cleveland, D. W. Pathways of spindle pole formation: different mechanisms; conserved components. J. Cell Biol., *138:* 953–956, 1997.
9. King, R. W., Deshaies. R. J., Peters, J. M., and Kirschner, M. W. How proteolysis drives the cell cycle. Science (Washington DC), *274:* 1652–1659, 1996.
10. King, R. W., Jackson, P. K., and Kirschner, M. W. Mitosis in transition. Cell, *79:* 563–571, 1994.
11. Hartwell, L. Defects in a cell cycle checkpoint may be responsible for the genomic instability of cancer cells. Cell, *71:* 543–546, 1992.
12. Seckinger, D., Sugarbaker, E., and Frankfurt, O. DNA content in human cancer. Application in pathology and clinical medicine. Arch. Pathol. Lab. Med., *113:* 619–626, 1989.
13. Barlogie, B., Drewinko, B., Schumann, J., Gohde, W., Dosik, G., Latreille, J., Johnston, D. A., and Freireich, E. J. Cellular DNA content as a marker of neoplasia in man. Am J. Med., *69:* 195–203, 1980.
14. Riley, R. S., Mahin, E. J., and Ross, W. DNA ploidy and cell cycle analysis. *In:* R. S. Riley, E. J. Mahin, and W. Ross (eds.), Clinical Applications of Flow Cytometry, pp. 251–323. New York: Igaku-Shoin, 1993.
15. Lengauer, C., Kinzler, K. W., and Vogelstein, B. Genetic instability in colorectal cancers. Nature (Lond.), *386:* 623–627, 1997.
16. Hartwell, L., Weinert, T., Kadyk, L., and Garvik, B. Cell cycle checkpoints, genomic instability and cancer. Cold Spring Harbor Symp. Quant. Biol., *59:* 259–263, 1994.

17. Mazia, D. The chromosome cycle and the centrosome cycle in the mitotic cycle. Int. Rev. Cytol., *100:* 49–92, 1987.
18. Fukasawa, K., Choi, T., Kuriyama, R., Rulong, S., and Vande Woude, G. F. Abnormal centrosome amplification in the absence of p53. Science (Washington DC), *271:* 1744–1747, 1996.
19. Doxsey, S. J., Stein, P., Evans, L., Calarco, P., and Kirschner, M. Pericentrin, a highly conserved protein of centrosomes involved in microtubule organization. Cell, *76:* 639–650, 1994.
20. Howard, R. B., Shroyer, K. R., Marcell, T., Swanson, L. E., Pagura, M. E., Mulvin, D. W., Cohen, M. E., and Johnston, M. R. Time-related effects of enzymatic disaggregation on model human lung carcinomas. Cytometry, *19:* 146–155, 1995.
21. Brown, R., Doxsey, S. J., Martin, R. L., and Welch, W. Molecular chaperones, hsp 70 and TCP-1, localize to centrosomes and affect microtubule growth. J. Biol. Chem., *271:* 824–832, 1996.
22. Norton, A. J., Jordan, S., and Yeomans, P. Brief, high-temperature heat denaturation: a simple and effective method of antigen retrieval for routinely processed tissues. J. Pathol., *173:* 371–379, 1994.
23. Hunyady, B., Krempels, K., Harta, K., and Mazcy, G. Immunohistochemical signal amplification by catalyzed reporter deposition and its application in double immunostaining. J. Histochem. Cytochem., *44:* 1353–1362, 1996.
24. Lichter, P., Boyle, A. L., Cremer, T., and Ward, D. Analysis of genes and chromosomes by nonisotopic *in situ* hybridization. Genet. Anal., *8:* 24–35, 1991.
25. Hunter, T. Oncoprotein networks. Cell, *88:* 333–346, 1997.
26. Purohit, A., and Doxsey, S. Spindle and nuclear abnormalities in cells overexpressing pericentrin. Mol. Biol. Cell, *8:* 171a, 1997.
27. Dick, J. E. Normal and leukemic human stem cells assayed in SCID mice. Sem. Immunol., *8:* 197–206, 1996.
28. Freedman, V. H., and Shin, S. I. Cellular tumorigenicity in nude mice: correlation with cell growth in semi-solid medium. Cell, *3:* 355–359, 1974.
29. Stanbridge, E. J., and Wilkinson, J. Analysis of malignancy in human cells: malignant and transformed phenotypes are under separate genetic control. Proc. Natl. Acad. Sci. USA, *75:* 1466–1469, 1978.
30. Winey, M. Genome instability: keeping the centrosome cycle on track. Curr. Biol., *6:* 962–964, 1996.
31. Pickett-Heaps, J. The evolution of the mitotic apparatus: an attempt at comparative ultrastructural cytology in dividing plant cells. Cytobios, *3:* 257–280, 1969.
32. Szollosi, D., Calarco, P., and Donahue, R. P. Absence of centrioles in the first and second meiotic spindles of mouse oocytes. J. Cell Sci., *11:* 521–541, 1972.
33. Debec, A., Szollosi, A., and Szollosi, D. A *Drosophila melanogaster* cell line lacking centrioles. Biol. Cell, *44:* 133–138, 1982.
34. Paulovich, A. G., Toczyski, D. P., and Hartwell, L. H. When checkpoints fail. Cell, *88:* 315–321, 1997.
35. Sluder, G., Miller F. J., and Rieder, C. L. The reproduction of centrosomes: nuclear *versus* cytoplasmic controls. J. Cell Biol., *103:* 1873–1881, 1986.
36. Sluder, G., Miller, F. J., Cole, R., and Rieder, C. L. Protein synthesis and the cell cycle: centrosome reproduction in sea urchin eggs is not under translational control. J. Cell Biol., *110:* 2025–2032, 1990.
37. Gard, D., Hafezi, S., Zhang, T., and Doxsey, S. J. Centrosome duplication continues in cycloheximide-treated *Xenopus* blastulae in the absence of a detectable cell cycle. J. Cell Biol., *110:* 2033–2042, 1990.
38. Lane, D. P. Cancer. p53, guardian of the genome. Nature (Lond.), *358:* 15–16, 1992.
39. Cross S. M., Sanchez, C. A., Morgan, C. A., Schimke, M. K., Ramel, S., Idzerda, R. L., Raskind, W. H., and Reid, B. J. A p53-dependent mouse spindle checkpoint. Science (Washington DC), *267:* 1353–1356, 1995.
40. Dictenberg, J., Zimmerman, W., Sparks, C., Young, A., Carrington, W., Zheng, Y., Vidair, C., Fay, F., and Doxsey, S. J. Pericentrin and γ-tubulin form a protein complex and are organized into a novel lattice at the centrosome. J. Cell Biol. *141:* 163–174, 1988.